The Hybrid Exposure of The Pierre Auger Observatory

P. Bernardini [1 2] C. Bleve[12 3] G. Cataldi[2], M. R. Coluccia[12], A. Corvaglia, [2] P. Creti,[2] S. D'amico[4 2], I. De Mitri[12], U. Giaccari[12], G. Mancarella[12], G. Marsella [42], D. Martello[12], M.Panareo[42], L.Perrone[42], C. Pinto[42], M. Settimo[12 5] and the AUGER Collaboration

[1]Dipartimento di Fisica, Università del Salento, Italy

[2]Istituto Nazionale di Fisica Nucleare sez. di Lecce, Italy,

[3]now at the Dept. of Physics, Bergische Universität Wuppertal, Germany ,

[4]Dipartimento di Ingegneria dell'Innovazione, Università del Salento, Italy

[5]now at the Dept. of Physics, University of Siegen, Germany ,

1. Introduction

Following ref.[1], we describe the determination of the hybrid exposure for events observed by the fluorescence telescopes in coincidence with at least one water-Cherenkov detector of the surface array. A detailed knowledge of the time dependence of the detection operations is crucial for an accurate evaluation of the exposure. We discuss the relevance of monitoring data collected during operations, such as the status of the fluorescence detector, background light and atmospheric conditions, that are used in both simulation and reconstruction.

2. Hybrid Ontime

The efficiency of fluorescence and hybrid data taking is influenced by many effects. These can be external, e.g. lightning or storms, or internal to the data taking itself, e.g. DAQ failures. For the determination of the *on-time* of the Pierre Auger Observatory in the hybrid detection mode it is therefore crucial to take into account all these occurrences and derive a solid description of the data taking time sequence.

Data losses and inefficiencies can occur on different levels, from the smallest unit of the FD, i.e. one single photomultiplier (pixel) readout channel, up to the highest level, i.e. the combined SD-FD data taking of the Observatory. To perform the time dependent detector simulation we have to take into account all known disturbances and then derive the on-time of the hybrid detection mode. To achieve this aim we rely on a variety of monitoring information and the data set itself. As a compromise between accuracy and stability we derived the complete detector status down to the single pixel for time intervals $T_{\rm bin} = 10$ min.

The time evolution of the full hybrid duty-cycle over 3 years during the construction phase of the observatory is shown in figure 1. It shows the

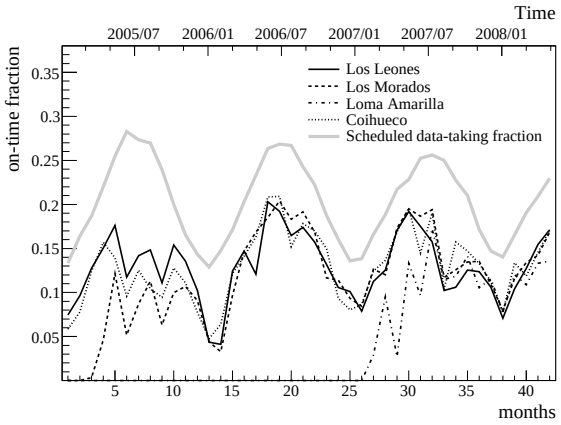

Figure 1. Time evolution of the average hybrid on-time fraction during the construction phase of the Pierre Auger Observatory. Both the seasonal modulation and the starting of commissioning phases of the different FD-sites are visible. Gray line represents the scheduled data-taking time fraction limited to the nights with moon-fraction lower than 60%.

on-time fraction, defined as the ratio of the overall on-time to the time duration of each interval. To avoid pile-up effects in the plot, time bins are chosen to coincide with FD data-taking shifts. Data-taking is currently limited to dark periods with moon-fractions smaller than 60% as seen by each individual telescope: this leads to about 16 nights of data taking per moon-cycle. The scheduled data-taking time fraction is also shown in figure 3 (gray line). A seasonal modulation is clearly visible, since higher fractions are observed in the austral winter during which the nights are longer. Note that the FD-site at Los Morados became operational in May 2005 and that at Loma Amarilla started in March 2007. After the ini-

tial phase of commissioning, the mean on-time is about 12% for all FD-sites, which corresponds roughly to about 70% of the scheduled time fraction. This efficiency is primarily due to weather effects with a minor part determined by detector effects.

3. Monte Carlo Simulations

For the calculation of the hybrid exposure, the size of the simulated event sample is crucial for acceptable statistical and systematic uncertainties. For this purpose the simulation activity followed a graded approach with full Monte Carlo analysis for specific studies, like the trigger efficiency, and fast simulations, validated with the full Monte Carlo method, when high statistics were required. A complete Monte Carlo hybrid simulation has been performed to study the trigger efficiency and the detector performance. The simulation sample consists of about 6000 proton and 3000 iron CORSIKA [2] showers with energies ranging between 10^{17} and $10^{19.5}$ eV. These energies are of particular interest for the trigger studies since they cover both SD and hybrid thresholds. The showers have been generated using respectively QGSJET-II [3,4] and FLUKA[5] as high and low energy hadronic interaction models. The FD simulation chain [6] reproduces in detail all the physical processes involved in the fluorescence technique. It includes the generation of fluorescence and Cherenkov photons in the atmosphere, their propagation through the atmosphere to the telescope aperture, the ray-tracing of photons in the Schmidt optics of the telescopes, and the simulation of the response of the electronics and of the multi-level trigger. The surface detector response is simulated using GEANT4 [7] within the framework provided by the Auger Offline software [8]. For this particular purpose we assume the SD array is fully operational and deployed. In figure 2 it is shown the hybrid trigger efficiency, i.e. the probability of detecting a fluorescence event in coincidence with at least one triggered SD station, is flat and equal to 1 at energies greater than 10^{18} eV, independent of primary mass. The difference between proton and iron primaries increases at lower energies but is negligible at energies as low as $10^{17.5}$ eV. Protons are slightly more efficient than iron primaries at the lowest energies. This is mainly due to the larger fraction of proton events interacting deeper in the atmosphere. The hybrid trigger efficiency from fluorescence data is also shown in figure 2. Only events landing on an active part of the surface detector have been selected and minimal quality cuts have been applied in order to have a reliable reconstructed energy and to safely derive the trigger probability curve. Data and simulation consistently show that a fluorescence event is always hybrid for energies larger than 10^{18} eV.

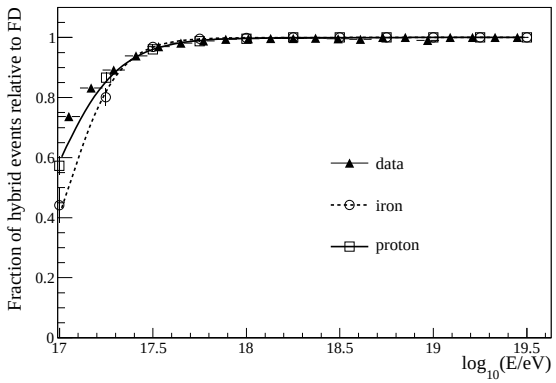

Figure 2. Relative hybrid trigger efficiency from hybrid simulation for proton and iron primaries. The hybrid trigger efficiency calculated using data is also shown.

In addition, the probability of a shower triggering a given SD station has been studied as a function of primary cosmic ray energy, mass, direction and distance to the shower axis, and a set of "Lateral Trigger Probability" (LTP) functions have been derived and parameterised. For a vertical proton primary shower, each station is on average fully efficient within a distance of 750, 1000, 1300, and 1600 m at energies of $10^{17.5}$ eV, 10^{18} eV, $10^{18.5}$ eV and 10^{19} eV, respectively. Details on this study are discussed in the following.

4. Lateral Trigger Probability functions

The LTP functions have been derived using detailed simulations of the EAS development and of the detector response. The simulation sample consists of about 15000 CORSIKA [2] showers (proton, iron and photon primaries) with zenith angle distributed as $\sin\theta\cos\theta$ (θ <65°) and energies ranging between 10^{17} and 10^{19} eV in steps of 0.25 in the logarithmic scale. A "thin sampling" mechanism at the level of 10^{-6} (optimal thinning) is applied following the standard method used for CORSIKA simulation with energies larger than 10^{16} eV [9]. The showers have been generated with the models QGSJETII [3] and FLUKA [5] for high and low energy hadronic interactions. In the simulation, the position of the shower core (i.e. the intersection of the shower axis with the ground) is uniformly distributed and each shower is used 5 times, each time with a different core position, in order to increase the statistics with a negligible degree of correlation. The surface detector response is simulated using GEANT4 [7]

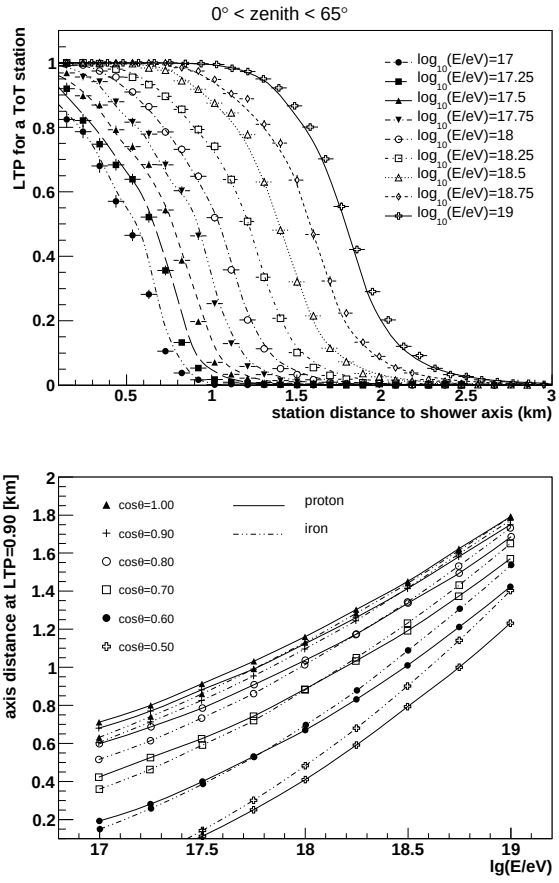

Figure 3. Top: Lateral Trigger Probability for a ToT station as a function of station distance to shower axis and for different energies (proton primary). The outcome of the parametrization is superimposed to simulation as a line. All zenith angles up to 65° are merged. Bottom: Axis distance at LTP =90% for proton and iron using the parametrization.

and adopting the sampling procedure to regenerate particles in a ground detector from thinned air shower simulations as described in [10]. The entire detector simulation is carried out within the framework provided by the Auger Offline software [8]. The trigger status of SD stations is inspected within a radius of 3 km from the shower axis and the Lateral Trigger Probability is derived. At distances larger than 3 km, the trigger efficiency is negligibly small for the class of events studied in this paper. All trigger modes of the surface detector are simulated in detail at all levels but at zenith angles less than 65°, the majority of events (with a negligible number of exceptions) are selected by the ToT condition. For moderately inclined showers, an asymmetry is expected in the signal detected in the stations placed at the same distance to the shower axis but with different azimuth in the shower frame [11]. Indeed, secondary particles arriving earlier, i.e. before the core reaches the ground, traverse less atmosphere and are less attenuated than the late ones. As a consequence, early stations may exhibit larger trigger probabilities and produce larger signals. Actually, for zenith angles below 65°, this effect has been found to have a quite low influence on the trigger probability, only noticeable above 30° (in simulations as well as in the data). In the following we consider LTP functions averaged over all the azimuths in the showers frame. A fit combining a step function (close to the axis) with an exponential (further away) reproduces reasonably well the full simulated data set. In Fig. 3 (top panel), the 1 ToT trigger probability from parametrization has been superimposed to simulation (proton primary, all zenith angles up to 65° are merged). The comparison is performed as in the following. For each simulated event, i.e. for a certain primary, energy and arrival direction, the LTP is calculated using the parametrization (lines) and shown together with the full simulation (points). The agreement is remarkably good in the entire energy range for proton (shown in the figure) and for iron and photon primaries. A summary view of the dependence of axis distance at LTP =90% on zenith and energy is shown in also in Fig. 3 (bottom panel), for proton and iron.

5. Fast simulation

To follow and reproduce the time dependence of the hybrid exposure, each detector configuration must be taken into account. This approach requires a large number of simulations. The method used to achieve this goal within a reasonable computational time relies on the simulation of longitudinal shower profiles generated with CONEX [12], a fast generator based on CORSIKA [2] shower code. After the simulation of the first few ultra-high energy interactions, CONEX switches to numerical solutions of the underlying cascade equations that describe the evolution of the different shower components. Although this method is extremely fast, the most important features provided by full Monte Carlo simulations, including shower to shower fluctuations, are very well reproduced [12,13].

The simulation of the FD response proceeds as in the full method discussed above. Since no ground level particles are generated by CONEX, the SD response cannot be directly simulated. In this case the SD trigger is reproduced using the LTP parameterisation functions. The actual status of the SD array is retrieved using the time of each simulated event. The event trigger probability is then calculated as the convolution of all the

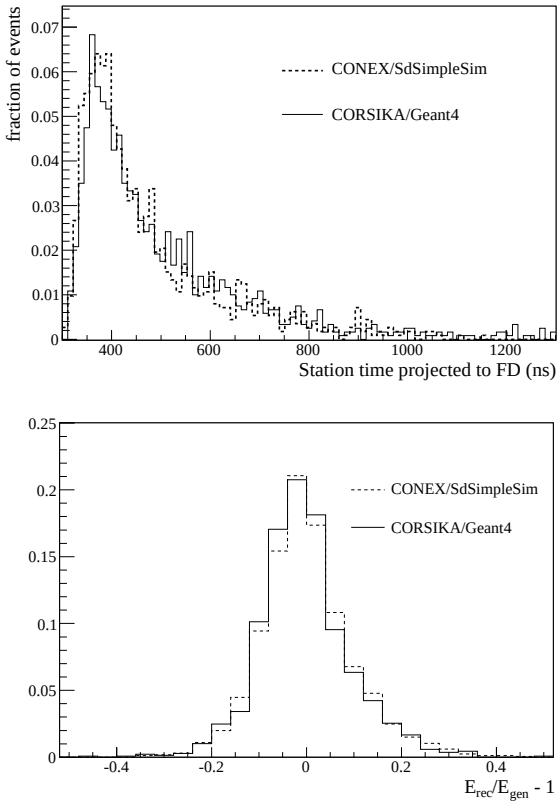

Figure 4. Comparison between CORSIKA/GEANT4 simulations and the fast CONEX/SdSimpleSim approach. (a): distribution of the time at which the SD station is triggered. (b): difference between the simulated and the reconstructed energies using the hybrid technique. The figures refer to events at $\log_{10}(E/eV) = 18.5$.

LTPs of the working SD stations. This is particularly important for low energy and inclined events.

The SD timing information needed in the hybrid reconstruction mode is provided by a simplified simulation (i.e. SdSimpleSim) implemented in the Offline simulation framework. With this approach the lateral distribution of the air shower is assumed to follow a NKG-like functional form [14,15]. A model generating realistic signal timing for the closest station to the shower axis has been derived from a full Monte Carlo using AIRES [16] simulations. The SdSimpleSim code also includes the simulation of noise triggered stations, which could spoil the reconstruction of the event. The noise rate of the surface detector is self-adjusting to yield 20 Hz per station. As a cross-check, the number of noise triggered stations has been derived from data and the obtained distributions have been parameterized.

Dedicated CORSIKA/GEANT4 simulations have been carried out to validate the performance of this fast approach against the full Monte Carlo method. Figure 4 shows the distribution of the station trigger times and the difference between simulated and reconstructed energy as obtained with the two simulation modes. The consistency between these results provides a robust validation of the fast approach and makes it possible to produce of huge number of simulated events.

6. Time Dependent Detector Simulation

The Monte Carlo simulation for the calculation of the hybrid exposure has been based on the fast simulation approach described above. In fact for covering all the energy ranges and the phase space of the detector configurations with enough statistical power, the number of simulated events is required to be largely oversampled with respect to the available raw data. The simulation has been designed to reproduce the actual sequencing of the detector status with a resolution of 10 minutes which corresponds to the time bin slot used for the on-time calculation. First a time is randomly chosen within the sidereal time interval we want to simulate. Then all the relevant status information about each detector is retrieved from the on-time calculations. Based on the on-time fraction during the simulated time bin, only a sub-sample of the events is sent to the detector simulation.

The CONEX showers used for this purpose have been generated from 10^{17} up to 10^{21} eV. QGSJET-II [3,4] and Sibyll [17] have been used as high energy interaction models. Proton and iron particles are taken as cosmic ray primaries.

To account for the growth of the array with time and problems during the SD data-taking, only the active SD stations are considered during simulation.

For the FD time dependent simulations the values of variance, baseline and trigger threshold averaged over 10 minutes are considered. The available FD absolute calibration data are used to adjust the simulated electronic gains on a pixel by pixel basis. This scales the shower signal with respect to the FADC trace noise and therefore influences the signal-to-noise ratio. In addition, incorrect cabling in some FD cameras is simulated for the instances discovered in the real detector. Data from the atmospheric monitoring system is used to set the hourly aerosol density profile as measured by the CLF [18] and the monthly mean molecular atmosphere as provided by balloon flights [19].

REFERENCES

1. J. Abraham *et al.* (The Pierre Auger Collaboration), Astroparticle Physics 34 (2011) 368-381
2. D. Heck *et al. Forschungszentrum Karlsruhe FZKA-6019*, 1998.
3. N. Kalmykov *et al.*, Nucl. Phys. B (Proc. Suppl.) 53 (1997) 17-28.
4. S. Ostapchenko, Nucl. Phys. B (Proc. Suppl.) 151 (2006) 143.
5. A. Fassò *et al.*, "FLUKA: a multi-particle transport code," *CERN-2005-10, INFN/TC_05/11, SLAC-R-773*, 2006.
6. L. Prado *et al.*, Nucl. Instrum. Meth. A545 (2005) 632.
7. S. Agostinelli *et al.* Nucl. Instr. and Meth. A506 (2003) 250.
8. S. Argirò *et al.*, Nucl. Instr. and Meth. A580 (2007).
9. D. Heck and J. Knapp, *Forschungszentrum Karlsruhe FZKA-6097*, 1998 http://www-ik.fzk.de/heck/publications/
10. P. Billoir, Astroparticle Physics 30 (2008), 270
11. M.T. Dova, M.E. Manceido, A.G. Mariazzi, H. Wahlberg, F. Arqueros D. Garca-Pinto Astropart. Phys. 31 (2009), 312
12. T. Bergmann *et al.*, Astropart. Phys. 26 (2007) 420-432.
13. T. Pierog *et al.*, *Proc. 30th Int. Cosmic Ray Conf.*, 2007.
14. K. Kamata and J. Nishimura Prog. Theoret. Phys. Suppl. 6 (1958) 93.
15. K. Greisen *Prog. Cosmic Rays Phys.*, vol. III, p. 26, 1965.
16. S. Sciutto *et al.*, "AIRES, a system for air shower simulation," *http://www.fisica.unlp.edu.ar/auger/aires*.
17. E.-J. Ahn, R. Engel, T. K. Gaisser, P. Lipari, and T. Stanev, Phys. Rev. D 80 (2009) 094003.
18. B. Fick *et al.*, Journal of Instrumentation (JINST) 1 (2006) 11003.
19. J. Abraham *et al.* (The Pierre Auger Collaboration), Astropart. Phys. 33 (2010) 108.